Int. J. Electrochem. Sci., 7 **(2012)** 4488 - 4497

International Journal of
ELECTROCHEMICAL
SCIENCE
www.electrochemsci.org

Electrooxidation of Ethanol on PtRh and PtRu Surfaces Studied in 0.5 M H_2SO_4: Relation to the Behaviour at Polycrystalline Pt

Boguslaw Pierozynski[*]

Department of Chemistry, Faculty of Environmental Protection and Agriculture, University of Warmia and Mazury in Olsztyn, Plac Lodzki 4, 10-957 Olsztyn, Poland
[*]E-mail: bogpierozynski@yahoo.ca

Received: 12 March 2012 / *Accepted:* 8 April 2012 / *Published:* 1 May 2012

The present study reports cyclic voltammetric and a.c. impedance spectroscopy investigations of electrooxidation process of ethanol on PtRh and PtRu catalyst surfaces, performed in 0.5 M H_2SO_4 supporting electrolyte. The kinetics of ethanol oxidation were examined in relation to those recently reported for polycrystalline Pt in the same test solution. Special consideration was given to the process of underpotential deposition (UPD) of H, as well as to temperature dependence of ethanol electrooxidation reaction on these two Pt-derived surfaces, studied over the temperature range 22-60 ^{o}C.

Keywords: Ethanol electrooxidation, UPD of H, Pt-based catalysts, temperature dependence, impedance spectroscopy.

1. INTRODUCTION

The most extensively studied alcohols for low-temperature PEMFC (*Proton Exchange Membrane Fuel Cell*) applications are methanol and ethanol fuels, where the latter one is considered a promising substitute for the former, due to its higher by about 30 % energy-density and non-toxic properties. Most importantly, ethanol is a renewable resource, which could conveniently be produced from a variety of available agricultural products and biomass substrates [1-4]. The process of electrooxidation of ethanol on a Pt-based catalyst surface is a multi-step anodic reaction, which could involve generation of numerous, surface-adsorbed reaction intermediates. However, it is widely accepted [2, 5, 6] that following the surface electrosorption step, ethanol molecule can either dissociate to surface-adsorbed CO_{ads} species, or else it could become electrooxidized to form acetaldehyde. Then, in the presence of adsorbed OH_{ads} species, successive oxidation steps lead to the formation of CO_2 or CH_3COOH, following their desorption from the catalyst surface. A large number of catalytic materials,

including bulk polycrystalline [3] and various single-crystal surfaces of Pt [3, 6-8], PtRu [2, 9], PtRh [2, 5], PtSn [1, 2, 8, 10-12] and PtPd [4] alloys/co-deposits, typically obtained on a carbon substrate, were examined towards their electrochemical behaviour in ethanol oxidation reaction.

This work represents a comprehensive electrochemical study of ethanol electrooxidation reaction on the selected Pt-based catalyst materials; namely, PtRh and PtRu alloy electrodes in 0.5 M H_2SO_4 supporting electrolyte. Kinetic characteristics of this process in relation to those recorded for polycrystalline Pt were discussed in detail. Special attention was given to the phenomenon of underpotential deposition of H, as well as to the temperature-dependence of ethanol oxidation reaction, in relation to the effects exhibited by polycrystalline Pt.

2. EXPERIMENTAL

2.1. Solutions and solutes, electrochemical cell and electrodes

Solutions were prepared from water derived from an 18.2 MΩ Direct- Q3 UV ultra-pure water purification system from Millipore. Aqueous 0.5 M H_2SO_4 solution was made up from sulphuric acid of highest purity available (SEASTAR Chemicals, Canada). Ethanol (Stanlab, pure, p.a., Poland) was used to prepare acidic solutions, at concentrations of 0.25 and 1.0 M C_2H_5OH. All solutions were de-aerated with high-purity argon (Ar 6.0 grade, Linde), prior to conducting electrochemical experiments.

An electrochemical cell made of Pyrex glass was used during the course of this work. The cell comprised three electrodes: a Pt-based alloy working electrode (WE), equipped with flexible adjustment (in a central part), a reversible Pd hydrogen electrode (RHE) as reference and a Pt counter electrode (CE), both in separate compartments. Prior to each series of experiments, the cell was taken apart and soaked in hot sulphuric acid for at least 3 hours. After having been cooled to about 40 ^oC, the cell was thoroughly rinsed with Millipore ultra-pure water. An identical procedure was applied for cleaning all the glassware used to prepare supporting electrolyte.

The palladium hydrogen electrode, acting as a reversible hydrogen electrode (RHE) was used throughout this work. The palladium RHE was made of a coiled Pd wire (0.5 mm diameter, 99.9 % purity, Aldrich) and sealed in soft glass. Before its use, this electrode was cleaned in hot sulphuric acid, followed by cathodic charging with hydrogen in 0.5 M H_2SO_4 (at current, I_c= 10 mA), until H_2 bubbles were clearly observed in the electrolyte. A counter electrode was made of a coiled Pt wire (1.0 mm diameter, 99.9998 % purity, Johnson Matthey, Inc.). Prior to its use, the counter electrode was cleaned in hot sulphuric acid. Pt/Rh alloy wire (Pt90/Rh10, 1 mm diameter, Goodfellow) and PtRu alloy foil (Pt95.2/Ru4.8, 0.05 mm thick, AlfaAesar) catalysts were used as working electrodes throughout this work.

2.2. Electrochemical equipment and procedures

Cyclic voltammograms were recorded at 22 ^oC and over the temperature range 22-60 ^oC (for the temperature-dependent experiments), at a sweep-rate of 50 mV s^{-1} by means of the *Solartron*

12,608 W Full Electrochemical System, consisting of 1260 frequency response analyzer (FRA) and 1287 electrochemical interface (EI). For a.c. impedance measurements, the 1260 FRA generator provided an output signal of 5 mVamplitude and the frequency range was typically swept between $1.0x10^5$ and $1.0x10^{-1}$ Hz. The instruments were controlled by *ZPlot 2.9* or *Corrware 2.9* software for Windows (Scribner Associates, Inc.). Presented impedance results were obtained through selection and analysis of representative series of experimental data. Usually, three impedance measurements were performed at each potential value. Reproducibility of such-obtained results was typically below 10 % from one measurement to another. The impedance data analysis was performed with *ZView 2.9* software package, where the spectra were fitted by means of a complex, non-linear, least-squares immitance fitting program, *LEVM 6*, written by Macdonald [13]. Three equivalent circuits for identified charge-transfer processes, including constant-phase elements (CPEs) to account for distributed capacitance were employed to analyze the obtained impedance results, as later shown in Figs. 3a to 3c.

3. RESULTS AND DISCUSSION

3.1. Cyclic voltammetry investigation of ethanol electrooxidation reaction

The cyclic voltammetric behaviour of ethanol electrooxidation reaction on PtRu and PtRh alloy electrodes in 0.5 M H_2SO_4 (examined at 0.25 and 1.0 M C_2H_5OH) is shown in Figs. 1a and 1b below, correspondingly.

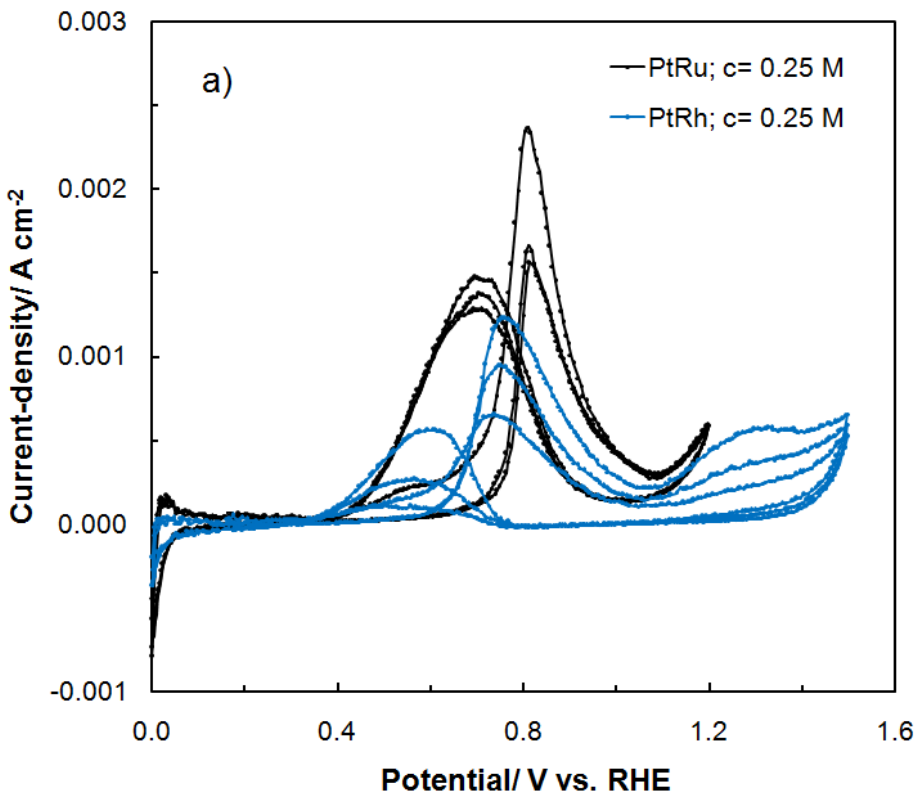

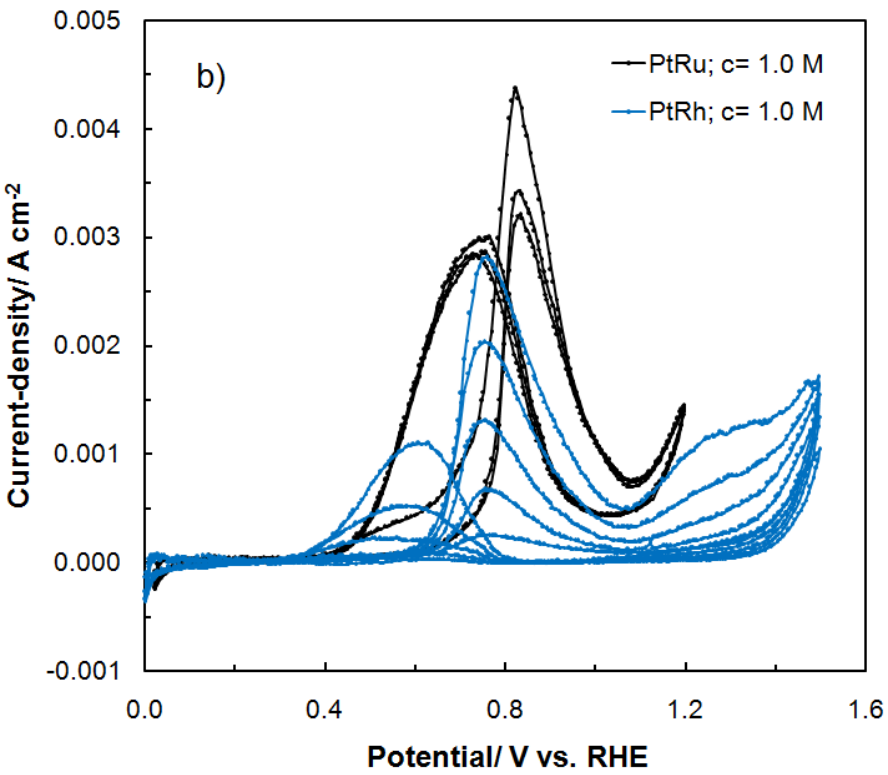

Figure 1. a) Cyclic voltammograms for ethanol electrooxidation on PtRu and PtRh alloy electrodes, carried-out in 0.5 M H_2SO_4, at a sweep-rate of 50 mV s^{-1} and in the presence of 0.25 M C_2H_5OH (three consecutive cycles were recorded for each CV run); b) As in Fig. 1a, but recorded at 1.0 M C_2H_5OH.

Similarly to the voltammetric effects recorded for polycrystalline Pt (see e.g. Fig. 1 in Ref. 14), two primary oxidation peaks appeared in the voltammetric profiles for both studied Pt-based alloys. Thus, for the PtRu electrode, an oxidation peak (centred at *ca*. 0.81 V) emerges in the CV profile upon an anodic sweep in Fig. 1a. Then, when the CV sweep is reversed towards the H_2 reversible potential, another anodic peak (centred at *ca*. 0.70 V vs. RHE) becomes revealed in the voltammetric profile. While the latter oxidation peak is usually attributed to the process of oxidation of surface-adsorbed CO_{ads} species, the former one is assigned in relevant literature to the formation of acetaldehyde on the catalyst surface [3, 6, 7]. On the other hand, the respective oxidation peaks recorded for the PtRh electrode were significantly (by *ca*. 100 and 50 mV) displaced towards less positive potentials (see Fig. 1a). Most importantly, the PtRh alloy catalyst exhibited considerably reduced voltammetric current-densities, as compared to those recorded for the PtRu electrode. The above could probably be explained in terms of weakening the Pt-CO bond in the presence of Ru [15], which results in significantly increased CO oxidation current-densities on the PtRu surface.

In addition, a four-fold increase of ethanol concentration in the supporting electrolyte gave rise to significantly magnified voltammetric current-densities (for both Pt-derived catalysts), which can clearly be observed in the corresponding voltammetric profiles of Fig. 1b.

3.2. Electrooxidation of ethanol by a.c. impedance spectroscopy

The a.c. impedance characteristics of the process of ethanol electrooxidation (in the presence of UPD of H) on PtRu and PtRh alloy catalysts in 0.5 M H_2SO_4 (at 0.25 M C_2H_5OH) are presented in Table 1 and Figs. 2a, and 2b below.

Table 1. Resistance and capacitance parameters for electrooxidation of ethanol (at 0.25 M C_2H_5OH) and UPD of H on PtRu and PtRh alloy electrodes in 0.5 M H_2SO_4 (at 22 ^oC), obtained by finding the equivalent circuits which best fitted the impedance data, as shown in Figs. 3a[a] through 3c[c].

E/ mV	R_H/ Ω cm^2	x10^6 C_{pH}/ F cm^{-2}s$^{\varphi 1-1}$	x10^6 C_{dl}/ F cm^{-2}s$^{\varphi 2-1}$	R_{ct}/ Ω cm^2
PtRu				
200[a]	11.7 ± 0.7	140.0 ± 12.2	38.8 ± 2.3	-----
300[b]	397.9 ± 35.8	9.1 ± 1.2	26.9 ± 1.3	184,580 ± 14,028
400[c]	-----	-----	18.2 ± 0.1	74,437 ± 603
500[c]	-----	-----	19.7 ± 0.1	11,033 ± 77
600[c]	-----	-----	64.8 ± 1.2	2,338 ± 35
700[c]	-----	-----	164.3 ± 8.2	1,327 ± 118
PtRh				
200[b]	37.1 ± 1.3	70.8 ± 3.1	28.0 ± 1.4	28,814 ± 1,095
300[b]	203.9 ± 8.4	12.2 ± 1.6	27.0 ± 2.3	19,972 ± 339
400[c]	-----	-----	30.9 ± 0.3	6,376 ± 77
500[c]	-----	-----	44.8 ± 0.5	1,949 ± 17
600[c]	-----	-----	69.5 ± 0.7	1,345 ± 12

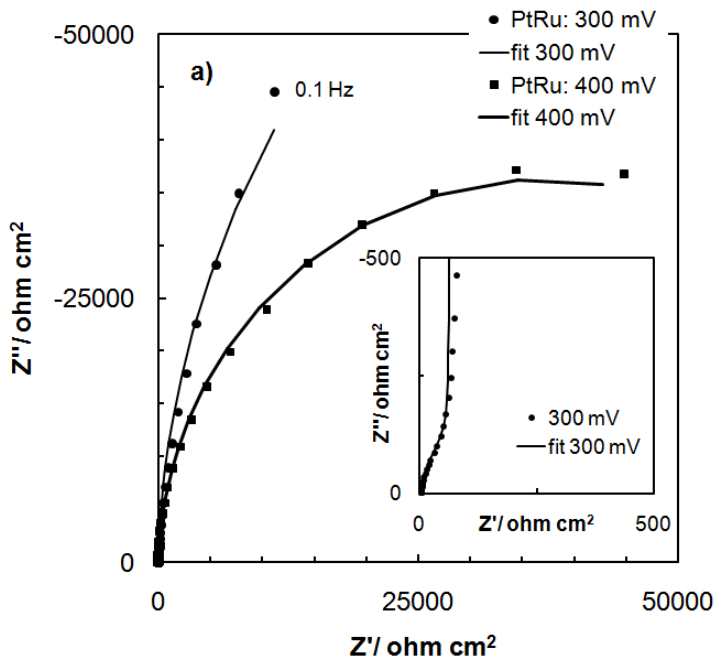

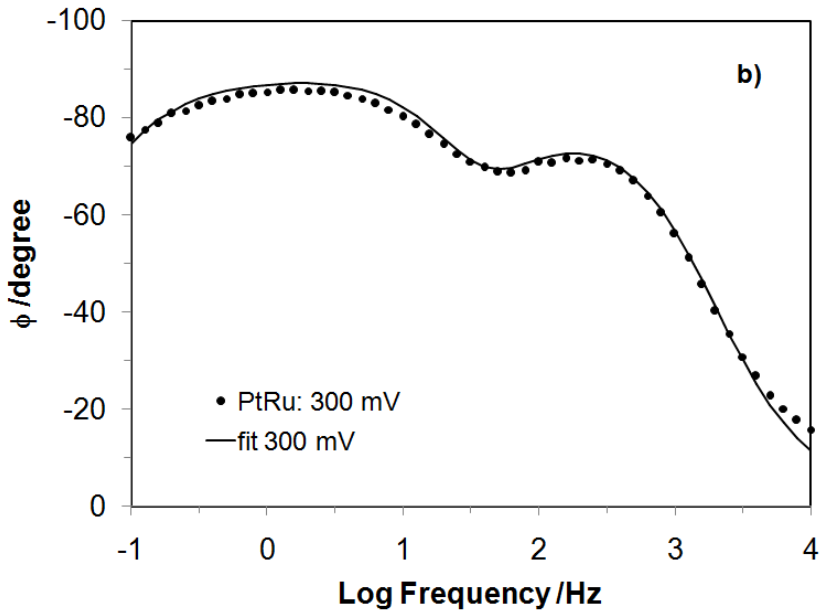

Figure 2. a) Complex-plane impedance plots for PtRu alloy electrode in contact with 0.5 M H_2SO_4, in the presence of 0.25 M C_2H_5OH, recorded at 300 and 400 mV vs. RHE (at 22 ^oC). The solid line corresponds to representation of the data according to the equivalent circuits shown in Figs. 3b and 3c; b) Bode phase-angle plot showing 2 maxima, observed over high and low frequency regions, recorded at 300 mV (other details as in Fig. 2a above).

Thus, for the PtRu electrode, the onset of ethanol oxidation can already be observed at 300 mV vs. RHE (Table 1), i.e. over the potential range for UPD of H. The recorded values of the charge-transfer resistance parameter (R_H) for the process of UPD of H (see Table 1) are of the same order as those recently reported for polycrystalline Pt (under analogous experimental conditions) by Pierozynski in Ref. 14. Please note that the recorded here rates for UPD of H are about 2 to 3 orders in magnitude slower than those typically reported for Pt, but in pure H_2SO_4 supporting electrolyte [16, 17]. Extremely high R_H resistance coincides with very low adsorption pseudocapacitance (C_{pH}) values (*ca*. 140 and 9 μF $cm^{-2}s^{\varphi 1-1}$ were recorded at 200, and 300 mV, correspondingly, see Table 1). This behaviour is very likely the result of significant interference from the adsorption of ethanol molecules, which process takes place in parallel with reversible deposition of H.

While the impedance performance at 200 mV represents typical behaviour for UPD of H, the Nyquist impedance spectrum recorded at 300 mV vs. RHE exhibited two partial, somewhat distorted semicircles (see an impedance spectrum obtained at 300 mV along with high frequency inset in Fig. 2a and a corresponding Bode phase angle plot in Fig. 2b). The smaller partial semicircle (see inset to Fig. 2a), observed only at high frequencies, corresponds to the process of UPD of H, and a large-diameter partial semicircle, observed throughout the intermediate frequency range, is associated with the charge-transfer process (R_{ct}) accompanying ethanol electrooxidation on the PtRu surface. Then, for the potential range 400-700 mV, a single partial semicircle (related to the process of ethanol electrooxidation) appears in the Nyquist impedance spectrum (see as an example the impedance spectrum recorded at 400 mV in Fig. 2a). Here, minimum of the charge-transfer resistance parameter

for ethanol oxidation: R_{ct} = 1,327 Ω cm^2 was recorded at 700 mV, near the peak current-density potential for the CV profile of PtRu catalyst in Fig. 1a.

Furthermore, the double-layer capacitance values (C_{dl}) exhibited oscillation from about 18 to nearly 65 μF $cm^{-2}s^{\varphi 2-1}$. Somewhat increased C_{dl} (over that commonly quoted value of 20 μF cm^{-2} for smooth and homogeneous surfaces [18, 19]) implies contribution from surface adsorption processes (e.g. involving reaction intermediates) that might take place over the corresponding potential range. A good example of this kind of behaviour makes the recorded at 700 mV C_{dl} value of 164.3 μF $cm^{-2}s^{\varphi 2-1}$). Also, a deviation from the purely capacitive behaviour (which necessitates the use of the CPE components in the equivalent circuits, see Figs. 3a through 3c) corresponds to dispersion of capacitance.

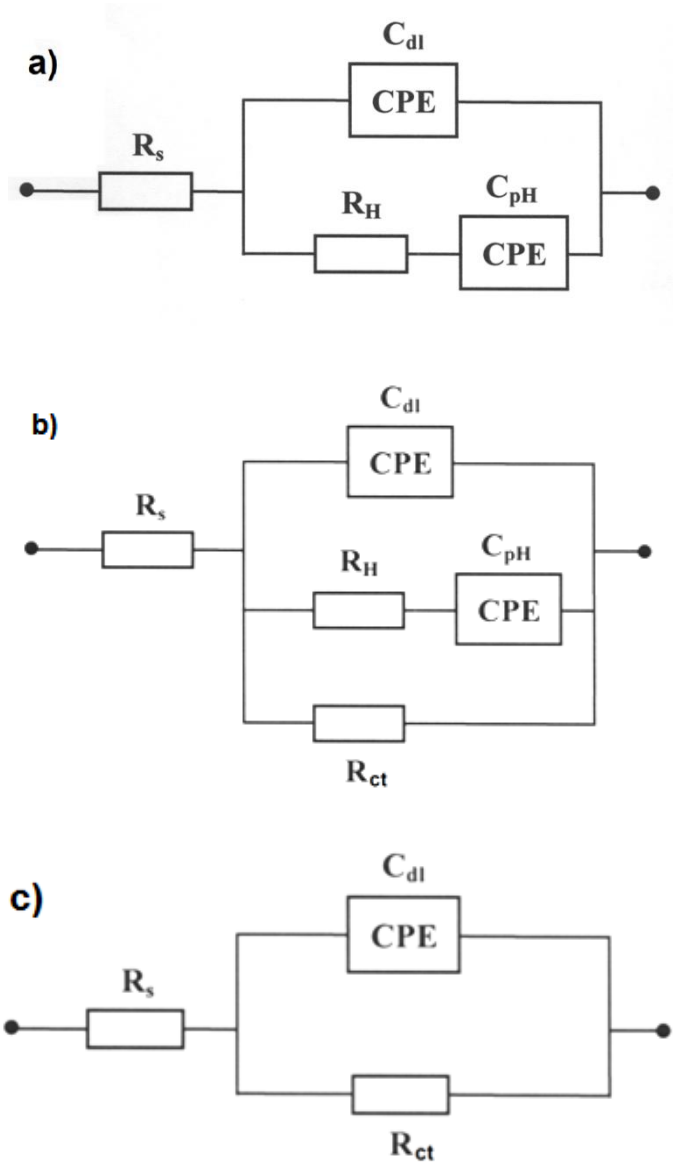

Figure 3. Three equivalent circuits, used for fitting the obtained a.c. impedance spectroscopy data in this work, where: R_s is solution resistance, C_{dl} is double-layer capacitance, R_H and C_{pH} are resistance and pseudocapacitance parameters for the process of UPD of H, R_{ct} is charge-transfer resistance parameter for electrooxidation of ethanol. The circuits include two constant phase elements (CPEs) to account for distributed capacitance.

This effect is typically assigned to slow ion adsorption-desorption processes [20] or to increasing surface inhomogeneity. The latter is likely a result of extended potentiostatic impedance measurements [20-22]. In this work, values of dimensionless parameters φ_1 and φ_2 (for the CPE components in Figs. 3a to 3c, where $0 \leq \varphi \leq 1$) oscillated between 0.87 and 0.98.

Similar impedance behaviour (also with respect to the kinetics of UPD of H) was observed at PtRh catalyst material. However, it can clearly be seen in Table 1 that ethanol electrooxidation reaction at the PtRh electrode becomes strongly facilitated (as compared to the behaviour at PtRu) for potentials, where the process actually commences, i.e. for the potential range 200-400 mV vs. RHE. Thus, the recorded "onset" values of the R_{ct} parameter came to 28,814 and 184,580 Ω cm^2 for the PtRh and PtRu catalysts, respectively. In fact, the ratio between the "onset" values of the charge-transfer resistance for the PtRh alloy and that recently reported for bulk polycrystalline Pt [14] came to about 0.27 (contrast to the behaviour at PtRu). These observations are in-line with the cyclic voltammetric behaviour observed in Fig. 1a, where the recorded voltammetric features for the PtRh electrode became considerably (by *ca*. 100 and 50 mV) shifted towards the H_2 reversible potential, as compared to those of the PtRu catalyst material. Thus, introduction of 10 % of rhodium into bulk Pt significantly facilitated the onset stage of ethanol electrooxidation reaction, being very likely the result of enhanced catalytic activity of Rh element towards breaking the C-C bond for electrosorbed ethanol molecules [5]. Again, the recorded in Table 1 double-layer capacitance values for the PtRh electrode oscillated between *ca*. 27 and 70 μF cm^{-2}s$^{\varphi 2-1}$, whereas those of the dimensionless parameters (φ_1 and φ_2) were between 0.83 and 0.98.

3.3. Temperature-dependence of ethanol electrooxidation reaction

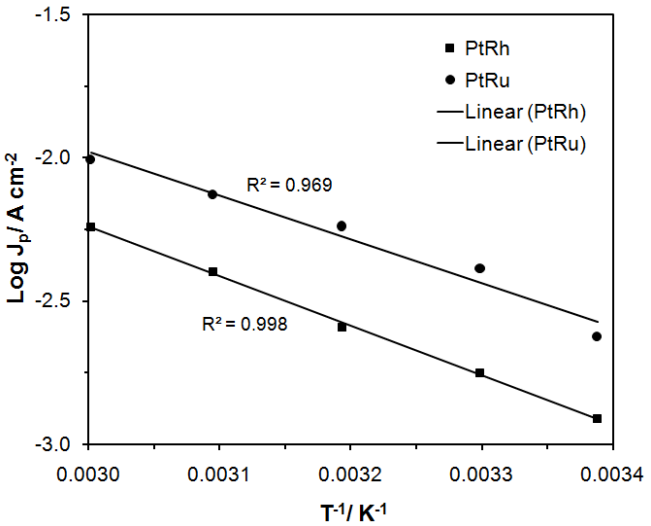

Figure 4. Arrhenius plots for ethanol electrooxidation (at 0.25 M C_2H_5OH) on PtRu and PtRh alloy electrodes in contact with 0.5 M H_2SO_4, recorded for the anodic peak current-density values.

Electrooxidation of ethanol on both examined Pt-based catalysts exhibited considerable temperature-dependence. Fig. 4 above presents Arrhenius plots for ethanol oxidation (at 0.25 M

C_2H_5OH) on the PtRu and PtRh alloy electrodes, recorded for the peak anodic current-density potential value, over the temperature range 22-60 ^oC. Thus, augmentation of the reaction temperature led to a significant increase of the recorded voltammetric oxidation current-densities. The Arrhenius plot-derived apparent activation energies (E_A) for electrooxidation of ethanol on the PtRu and PtRh catalyst materials came to 29.2 and 33.0 kJ mol^{-1}, correspondingly, where the latter one was very close to that recently reported for bulk polycrystalline Pt material by the author of this work in Ref. 14.

4. CONCLUSIONS

The presence of 10 % of Rh in Pt-based binary catalyst material significantly affects the kinetics of ethanol oxidation reaction (performed in H_2SO_4 supporting electrolyte) at its initial phase. The above results from enhanced catalytic properties of rhodium towards breaking the C-C bond for electrosorbed ethanol molecules. Otherwise, the kinetics of ethanol oxidation reaction on PtRh and PtRu alloys in H_2SO_4 are comparable with those reported on a polycrystalline Pt electrode under similar experimental conditions. The onset of ethanol electrooxidation at both examined Pt-based catalysts extends over the potential range characteristic to the reversible deposition (UPD) of H on Pt. The presence of ethanol molecules (or reaction intermediates) on the surface of PtRu (or PtRh) catalyst dramatically affects the rates for UPD of H, slowing them down by several orders in magnitude, as compared to those obtained in the absence of ethanol in the supporting electrolyte. In addition, the kinetics of ethanol electrooxidation on PtRu and PtRh alloy materials revealed strong temperature dependence, where the derived apparent energies of activation approached those reported for polycrystalline Pt.

ACKNOWLEDGEMENTS
This work has been financed by the strategic program of the National (Polish) Centre for Research and Development (NCBiR): *„Advanced Technologies for Energy Generation. Task 4: Elaboration of Integrated Technologies for the Production of Fuels and Energy from Biomass, Agricultural Waste and other Waste Materials”*.

References

1. S. Rousseau, C. Coutanceau, C. Lamy and J.M. Leger, *J. Power Sources*, 158 (2006) 18.
2. S.Q. Song, W.J. Zhou, Z.H. Zhou, L.H. Jiang, G.Q. Sun, Q. Xin, V. Leontidis, S. Kontou and P. Tsiakaras, *Int. J. Hydrogen Energy*, 30 (2005) 995.
3. A.A. Abd-El-Latif, E. Mostafa, S. Huxter, G. Attard and H. Baltruschat, *Electrochim. Acta*, 55 (2010) 7951.
4. S.S. Mahapatra, A. Dutta and J. Datta, *Electrochim. Acta*, 55 (2010) 9097.
5. S.S. Gupta and J. Datta, *J. Electroanal. Chem*., 594 (2006) 65.
6. X.H. Xia, H.D. Liess and T. Iwasita, *J. Electroanal. Chem*., 437 (1997) 233.
7. J.F. Gomes, B. Busson, A. Tadjeddine and G. Tremiliosi-Filho, *Electrochim. Acta*, 53 (2008) 6899.
8. A.A. El-Shafei and M. Eiswirth, *Surf. Sci*., 604 (2010) 862.

9. N. Fujiwara, Z. Siroma, S. Yamazaki, T. Ioroi, H. Senoh and K. Yasuda, *J. Power Sources*, 185 (2008) 621.
10. S.S. Gupta, S. Singh and J. Datta, *Mat. Chem. Phys*., 120 (2010) 682.
11. E.E. Switzer, T.S. Olson, A.K. Datye, P. Atanassov, M.R. Hibbs and C.J. Cornelius, *Electrochim. Acta*, 54 (2009) 989.
12. F.C. Simoes, D.M. dos Ajnos, F. Vigier, J.M. Leger, F. Hahn, C. Coutanceau, E.R. Gonzalez, G. Tremiliosi-Filho, A.R. de Andrade, P. Olivi and K.B. Kokoh, *J. Power Sources*, 167 (2007) 1.
13. J. R. Macdonald, *Impedance Spectroscopy, Emphasizing Solid Materials and Systems*, John Wiley & Sons, Inc., New York, (1987).
14. B. Pierozynski, *Int. J. Electrochem. Sci*., 7 (2012) (in press).
15. G. Wu, L. Li and B.Q. Xu, *Electrochim. Acta*, 50 (2004) 1.
16. S. Morin, H. Dumont and B.E. Conway, *J. Electroanal. Chem.*, 412 (1996) 39.
17. B.E. Conway and B. Pierozynski, *J. Electroanal. Chem.*, 622 (2008) 10.
18. A. Lasia and A. Rami, *J. Applied Electrochem*., 22 (1992) 376.
19. L. Chen and A. Lasia, *J. Electrochem. Soc*., 138 (1991) 3321.
20. T. Pajkossy, *J. Electroanal. Chem.*, 364 (1994) 111.
21. B.E. Conway in *Impedance Spectroscopy. Theory, Experiment, and Applications*, E. Barsoukov and J. Ross Macdonald (Eds.), Wiley-Interscience, John Wiley & Sons, Inc., Hoboken, N.J., 4.5.3.8 (2005) 494.
22. W.G. Pell, A. Zolfaghari and B.E. Conway, *J. Electroanal. Chem*., 532 (2002) 13.

© 2012 by ESG (www.electrochemsci.org)